

The influence of the scalar unparticle on the W - pair production at ILC in the Randall Sundrum model

Dang Van Soa^{a,1}, Bui Thi Ha Giang^b

^a Hanoi Metropolitan University, 98 Duong Quang Ham, Hanoi, Vietnam

^b Hanoi National University of Education, 136 Xuan Thuy, Hanoi, Vietnam

Abstract

An attempt is made to present the contribution of the scalar unparticle on some scattering processes in the Randall - Sundrum (RS) model. We have evaluated the contribution of the scalar unparticle on the W - pair production cross-sections at International Linear Colliders (ILC). Numerical evaluations show that the cross section of the W - pair production depends strongly on the collision energy \sqrt{s} , the scaling dimension d_U of the unparticle operator \mathcal{O}_U and also the energy scale Λ_U . The results indicate that with the influence of the scalar unparticle, the cross-sections for the W - pair production are enhanced and much larger than the pair production of scalar particles (Higgs/radion) under the same conditions, which may give observable values at ILC. It is worth noting that the W mode at ILC is possible to discover the existence of the unparticle with the low values of the scaling dimension and the bounds on scale Λ_U are around few TeV .

Keywords: scalar unparticle, Randall-Sundrum model, ILC.

I Introduction

The Standard model (SM) is very successful in describing the particle physics. In the Lagrangian of the Standard model, the scale invariance is broken at or above the electroweak scale [1, 2]. At TeV scale, the scale invariant sector has been considered as an effective theory and that if it exists, it is made of unparticle suggested by Geogri [3, 4]. Based on the Banks-Zaks theory [5, 6], unparticle stuff with nontrivial scaling dimension is considered to exist in our world and this opens a window to test the effects of the possible scalar invariant sector, experimentally. Recently, the possibility of the unparticle has been studied with CMS detector at the LHC [7, 8].

The effects of unparticle on properties of high energy colliders have been intensively studied in Refs. [9–19]. In the rest of this work, we restrict ourselves by considering only scalar unparticle. The scalar unparticle propagator is given by [2, 4, 20]

$$\Delta_{scalar} = \frac{iA_{d_U}}{2\sin(d_U\pi)}(-q^2)^{d_U-2}, \quad (1)$$

where

$$A_{d_U} = \frac{16\pi^2\sqrt{\pi}}{(2\pi)^{2d_U}} \frac{\Gamma\left(d_U + \frac{1}{2}\right)}{\Gamma(d_U - 1)\Gamma(2d_U)}, \quad (2)$$

$$(-q^2)^{d_U-2} = \begin{cases} |q^2|^{d_U-2} e^{-d_U\pi} & \text{for s-channel process, } q^2 \text{ is positive,} \\ |q^2|^{d_U-2} & \text{for u-, t-channel process, } q^2 \text{ is negative.} \end{cases} \quad (3)$$

The effective interactions for the scalar unparticle operators are given by

$$\lambda_{ff} \frac{1}{\Lambda_U^{d_U-1}} \bar{f} f O_U, \lambda_{gg} \frac{1}{\Lambda_U^{d_U}} G_{\alpha\beta} G^{\alpha\beta} O_U, \quad (4)$$

¹soadangvan@gmail.com

where $G^{\alpha\beta}$ denotes the gauge field strength and f stands for a standard model fermion.

In our previous work [20], we have evaluated the contribution of scalar unparticle on the production of Higgs - radion at high energy colliders in the RS model. In this work, we will study the influence of the scalar unparticle on the W - pair production at ILC in the RS model. Various ILC physics studies can have a great impact on understanding a new physics around TeV scale. Moreover, it can be transformed into $\gamma\gamma$ collisions with the photon beams generated by using the Compton backscattering of the initial electron and laser beams. The photon collider would open a wider window to probe new physics beyond the SM.

The layout of this paper is as follows. In Section II, we give Feynman rules for the couplings of Higgs/radion and scalar unparticle in the RS model. The influence of the scalar unparticle on the W - pair production at ILC is calculated in Section III. Finally, we summarize our results and make conclusions in Section IV.

II Feynman rules for the couplings of Higgs/radion and scalar unparticle in the RS model

The RS model involves two three-branes bounding a slice of 5D compact anti-de Sitter space. Gravity is localized at the UV brane, while the SM fields are supposed to be localized at the IR brane [21]. The separation between the two 3-branes leads directly to the existence of an additional scalar called the radion (ϕ), corresponding to the quantum fluctuations of the distance between the two 3-branes. Radion and Higgs boson have the same quantum numbers. General covariance allows a possibility of mixing between the radion and the Higgs boson. The gravity-scalar mixing is described by the following action [22]

$$S_\xi = \xi \int d^4x \sqrt{g_{vis}} R(g_{vis}) \hat{H}^+ \hat{H}, \quad (5)$$

where ξ is the mixing parameter, $R(g_{vis})$ is the Ricci scalar for the metric $g_{vis}^{\mu\nu} = \Omega_b^2(x)(\eta^{\mu\nu} + \varepsilon h^{\mu\nu})$ induced on the visible brane, $\Omega_b(x) = e^{-kr_c\pi}(1 + \frac{\phi_0}{\Lambda_\phi})$ is the warp factor, ϕ_0 is the canonically normalized massless radion field, \hat{H} is the Higgs field in the 5D context before rescaling to canonical normalization on the brane. The mixing of Higgs-radion was given detailly in Refs. [22, 23]. Feynman rules for the couplings of Higgs/radion and the scalar unparticle are showed as follows

$$g_{f\bar{f}h} = i\bar{g}_{f\bar{f}h} = -i \frac{gm_f}{2m_W} (d + \gamma b), \quad (6)$$

$$g_{f\bar{f}\phi} = i\bar{g}_{f\bar{f}\phi} = -i \frac{gm_f}{2m_W} (c + \gamma a), \quad (7)$$

$$\begin{aligned} g_{WW_h} &= i\bar{g}_{WW_h} [\eta^{\mu\nu} - 2g_h^W ((k_1 k_2) \eta^{\mu\nu} - k_1^\nu k_2^\mu)] \\ &= igm_W (d + \gamma b - \gamma b \kappa_W) [\eta^{\mu\nu} - 2g_h^W ((k_1 k_2) \eta^{\mu\nu} - k_1^\nu k_2^\mu)], \end{aligned} \quad (8)$$

$$\begin{aligned} g_{WW_\phi} &= i\bar{g}_{WW_\phi} [\eta^{\mu\nu} - 2g_\phi^W ((k_1 k_2) \eta^{\mu\nu} - k_1^\nu k_2^\mu)] \\ &= igm_W (c + \gamma a - \gamma a \kappa_W) [\eta^{\mu\nu} - 2g_\phi^W ((k_1 k_2) \eta^{\mu\nu} - k_1^\nu k_2^\mu)], \end{aligned} \quad (9)$$

$$\begin{aligned} g_{\gamma\gamma h} &= iC_{\gamma h} [(k_1 k_2) \eta^{\mu\nu} - k_1^\nu k_2^\mu] \\ &= -i \frac{\alpha}{2\pi v_0} \left((d + \gamma b) \sum_i e_i^2 N_c^i F_i(\tau_i) - (b_2 + b_Y) \gamma b \right) \\ &\quad \times [(k_1 k_2) \eta^{\mu\nu} - k_1^\nu k_2^\mu], \end{aligned} \quad (10)$$

$$\begin{aligned}
g_{\gamma\gamma\phi} &= iC_{\gamma\phi} [(k_1 k_2)\eta^{\mu\nu} - k_1^\nu k_2^\mu] \\
&= -i\frac{\alpha}{2\pi v_0} \left((c + \gamma a) \sum_i e_i^2 N_c^i F_i(\tau_i) - (b_2 + b_Y)\gamma a \right) \\
&\quad \times [(k_1 k_2)\eta^{\mu\nu} - k_1^\nu k_2^\mu],
\end{aligned} \tag{11}$$

$$g_{f\bar{f}U} = i\bar{g}_{f\bar{f}U} = i\frac{\lambda_{ff}}{\Lambda_U^{d_U-1}}, \tag{12}$$

$$g_{\gamma\gamma U} = -i\bar{g}_{\gamma\gamma U} [(p_1 p_2)\eta^{\mu\nu} - p_1^\nu p_2^\mu] = -4i\frac{\lambda_{\gamma\gamma}}{\Lambda_U^{d_U}} [(p_1 p_2)\eta^{\mu\nu} - p_1^\nu p_2^\mu], \tag{13}$$

$$g_{WWU} = -i\bar{g}_{WWU} [(p_1 p_2)\eta^{\mu\nu} - p_1^\nu p_2^\mu] = -4i\frac{\lambda_{WW}}{\Lambda_U^{d_U}} [(p_1 p_2)\eta^{\mu\nu} - p_1^\nu p_2^\mu]. \tag{14}$$

Here $\gamma = v/\Lambda_\phi$, $v = 246$ GeV, $a = -\frac{\cos\theta}{Z}$, $b = \frac{\sin\theta}{Z}$, $c = \sin\theta + \frac{6\xi\gamma}{Z}\cos\theta$, $d = \cos\theta - \frac{6\xi\gamma}{Z}\sin\theta$, θ is the mixing angle, $g_h^W = \frac{\gamma b}{(d + \gamma b - \kappa_W \gamma b)m_W^2} \left(\frac{1}{2kb_0} + \frac{\alpha b_2}{8\pi \sin^2\theta_W} \right)$, $g_\phi^W = \frac{\gamma a}{(c + \gamma a - \kappa_W \gamma a)m_W^2} \left(\frac{1}{2kb_0} + \frac{\alpha b_2}{8\pi \sin^2\theta_W} \right)$, $\kappa_W = \frac{3m_W^2 kb_0}{2\Lambda_\phi^2 (k/M_{Pl})^2}$, $\frac{1}{2}kb_0 \sim 35$ [23], $b_3 = 7$, $b_2 = 19/6$, $b_Y = -41/6$, θ_W stands for the Weinberg angle. The auxiliary functions of the h and ϕ are given by

$$F_{1/2}(\tau_i) = -2\tau_i[1 + (1 - \tau_i)f(\tau_i)], \tag{15}$$

$$F_1(\tau_i) = 2 + 3\tau_i + 3\tau_i(2 - \tau_i)f(\tau_i), \tag{16}$$

with

$$f(\tau_i) = \left(\sin^{-1} \frac{1}{\sqrt{\tau_i}} \right)^2 \quad (\text{for } \tau_i > 1), \tag{17}$$

$$f(\tau_i) = -\frac{1}{4} \left(\ln \frac{\eta_+}{\eta_-} - i\pi \right)^2 \quad (\text{for } \tau_i < 1), \tag{18}$$

$$\eta_\pm = 1 \pm \sqrt{1 - \tau_i}, \quad \tau_i = \left(\frac{2m_i}{m_s} \right)^2. \tag{19}$$

Here, m_i is the mass of the internal loop particle (including quarks, leptons and W boson), m_s is the mass of the scalar state (h or ϕ), $\tau_f = \left(\frac{2m_f}{m_s} \right)^2$, $\tau_W = \left(\frac{2m_W}{m_s} \right)^2$ denote the squares of fermion and W gauge boson mass ratios, respectively.

III The influence of the scalar unparticle on the W - pair production at ILC

An investigation of W-pair production at ILC play an important role in testing the SM and searching for physics beyond. In our previous work [20], we have evaluated the contribution of scalar unparticle on the production of Higgs - radion at high energy colliders in RS model. In this work, we will evaluate the influence of the scalar unparticle on the W - pair production at ILC, including the $e^+e^- \rightarrow W^+W^-$ process and the $\gamma\gamma \rightarrow W^+W^-$ subprocess.

1. The $e^+e^- \rightarrow W^+W^-$ collision

Firstly, we consider the collision process in which the initial state contains electron and positron, the final state contains a pair of W^- and W^+ through the scalar propagators (ϕ, h, U),

$$e^-(p_1) + e^+(p_2) \xrightarrow{\phi, h, U} W^-(k_1) + W^+(k_2). \quad (20)$$

The transition amplitude is given by

$$\begin{aligned} M_{fi} = & i \frac{\bar{g}_{ee\phi} \bar{g}_{W\phi}}{q^2 - m_\phi^2} \bar{v}(p_2) u(p_1) \varepsilon_\mu^*(k_1) [\eta^{\mu\nu} - 2g_\phi^W ((k_1 k_2) \eta^{\mu\nu} - k_1^\nu k_2^\mu)] \varepsilon_\nu^*(k_2) \\ & + i \frac{\bar{g}_{eeh} \bar{g}_{Wh}}{q^2 - m_h^2} \bar{v}(p_2) u(p_1) \varepsilon_\mu^*(k_1) [\eta^{\mu\nu} - 2g_h^W ((k_1 k_2) \eta^{\mu\nu} - k_1^\nu k_2^\mu)] \varepsilon_\nu^*(k_2) \\ & + i \bar{g}_{eeU} \bar{g}_{WU} \frac{A_{dU}}{2 \sin(d_U \pi)} (-q^2)^{d_U - 2} \bar{v}(p_2) u(p_1) \varepsilon_\mu^*(k_1) [(k_1 k_2) \eta^{\mu\nu} - k_1^\nu k_2^\mu] \varepsilon_\nu^*(k_2). \end{aligned} \quad (21)$$

Here, $q = p_1 + p_2 = k_1 + k_2$, $s = (p_1 + p_2)^2$ is the square of the collision energy.

From the expressions of the differential cross-section [24]

$$\frac{d\sigma}{d(\cos\psi)} = \frac{1}{32\pi s} \frac{|\vec{k}_1|}{|\vec{p}_1|} |M_{fi}|^2, \quad (22)$$

where $\psi = (\vec{p}_1, \vec{k}_1)$ is the scattering angle. The model parameters are chosen as $\lambda_{ff} = \lambda_{WW} = \lambda_0 = 1$, $m_h = 125$ GeV, $m_\phi = 10$ GeV [25]. As shown in [20], the cross section is flat when $d_U > 1.6$, therefore we choose the d_U as $1 < d_U < 1.5$. We give estimates for the cross-sections as follows

i) In Fig.1, the total cross-section is plotted as the function of P_{e^-}, P_{e^+} , which are the polarization coefficients of e^-, e^+ beams, respectively. The parameters are chosen as $\sqrt{s} = 500$ GeV, $d_U = 1.1$, $\Lambda_U = 1000$ GeV. The figure indicates that the total cross-section achieves the minimum value when $P_{e^-} = P_{e^+} = \pm 1$ and the maximum value when $P_{e^-} = 1, P_{e^+} = -1$ or $P_{e^-} = -1, P_{e^+} = 1$.

ii) In Fig.2, the total cross-section is plotted as the function of d_U in case of $P_{e^-} = 1, P_{e^+} = -1$. The parameters are chosen as $\sqrt{s} = 500$ GeV, $\Lambda_U = 1000$ GeV. From the figure we can see that the cross section decreases rapidly as d_U increases.

iii) In Fig.3, we evaluate the dependence of the total cross-section on the collision energy \sqrt{s} in case of $P_{e^-} = 1, P_{e^+} = -1$. The collision energy is chosen in the range of $500 \text{ GeV} \leq \sqrt{s} \leq 1000$ GeV (ILC). The parameters are chosen as $d_U = 1.1$, $\Lambda_U = 1000$ GeV. The figure shows that the total cross-section increases rapidly when the collision energy \sqrt{s} increases.

iv) In Fig.4, we evaluate the dependence of the total cross-section on the Λ_U at the fixed collision energy, $\sqrt{s} = 500$ GeV. The polarization coefficients are chosen as $P_{e^-} = 1, P_{e^+} = -1$. In case of the additional scalar unparticle propagator, the cross-section decreases rapidly in the region of $1 \text{ TeV} \leq \Lambda_U \leq 3 \text{ TeV}$.

Some numerical values for cross sections in the case of $d_U = 1.1$ are given detaily in Table 1. The results show that the cross-sections are about 10^{11} times larger than that of the W^- pair production without the scalar unparticle propagator under the same conditions.

2. The $\gamma\gamma \rightarrow W^-W^+$ subprocess

Now we consider the collision process in which the initial state contains the couple of photons, the final state contains the pair of W^- and W^+ ,

$$\gamma(p_1) + \gamma(p_2) \xrightarrow{\phi, h, U} W^-(k_1) + W^+(k_2). \quad (23)$$

The transition amplitude is given by

$$\begin{aligned}
M_{fi} = & -i \frac{C_{\gamma\phi}\bar{g}_{W\phi}}{q^2 - m_\phi^2} \varepsilon_\mu(p_1) [(p_1 p_2) \eta^{\mu\nu} - p_1^\nu p_2^\mu] \varepsilon_\nu(p_2) \varepsilon_\rho^*(k_1) [\eta^{\rho\sigma} - 2g_\phi^W ((k_1 k_2) \eta^{\rho\sigma} - k_1^\sigma k_2^\rho)] \varepsilon_\sigma^*(k_2) \\
& -i \frac{C_{\gamma h}\bar{g}_{Wh}}{q^2 - m_h^2} \varepsilon_\mu(p_1) [(p_1 p_2) \eta^{\mu\nu} - p_1^\nu p_2^\mu] \varepsilon_\nu(p_2) \varepsilon_\rho^*(k_1) [\eta^{\rho\sigma} - 2g_h^W ((k_1 k_2) \eta^{\rho\sigma} - k_1^\sigma k_2^\rho)] \varepsilon_\sigma^*(k_2) \\
& + i \bar{g}_{\gamma\gamma U} \bar{g}_{WWU} \frac{A_{d_U}}{2 \sin(d_U \pi)} (-q^2)^{d_U - 2} \varepsilon_\mu(p_1) [(p_1 p_2) \eta^{\mu\nu} - p_1^\nu p_2^\mu] \varepsilon_\nu(p_2) \varepsilon_\rho^*(k_1) [(k_1 k_2) \eta^{\rho\sigma} - k_1^\sigma k_2^\rho] \varepsilon_\sigma^*(k_2).
\end{aligned} \tag{24}$$

The effective cross-section $\sigma(s)$ for the $\gamma\gamma \rightarrow W^- W^+$ subprocess at the ILC can be calculated as follows

$$\sigma_{sub}(s) = \int_{4m_W^2/s}^{0.83} dx f_{\gamma/e}(x) \int_{(\cos\psi)_{min}}^{(\cos\psi)_{max}} d\cos\psi \frac{d\hat{\sigma}(\hat{s})}{d\cos\psi}, \tag{25}$$

where $x = \hat{s}/s$ in which $\sqrt{\hat{s}}$ is center of mass energy of the $\gamma\gamma \rightarrow W^- W^+$ subprocess, \sqrt{s} is center of mass energy of the ILC, $x_{max} = \frac{\zeta}{1+\zeta}$. The photon distribution function $f_{\gamma/e}$ is given by [26]

$$f_{\gamma/e} = \frac{1}{D(\zeta)} \left[(1-x) + \frac{1}{1-x} - \frac{4x}{\zeta(1-x)} + \frac{4x^2}{\zeta^2(1-x)^2} \right], \tag{26}$$

where

$$D(\zeta) = \left(1 - \frac{4}{\zeta} - \frac{8}{\zeta^2} \right) \ln(1+\zeta) + \frac{1}{2} + \frac{8}{\zeta} - \frac{1}{2(1+\zeta)^2}. \tag{27}$$

For $\zeta = 4.8$, $x_{max} = 0.83$. We estimate the production cross-sections with the contribution of the scalar unparticle propagator as follows

i) In Fig.5, the total cross-section is plotted as the function of d_U . The parameters are chosen as $\sqrt{s} = 500$ GeV, $\Lambda_U = 1000$ GeV. From the figure we can see that the cross section decreases rapidly as d_U increases.

ii) In Fig.6, we evaluate the dependence of the total cross-section on the collision energy \sqrt{s} . The collision energy is chosen in the range of $500 \text{ GeV} \leq \sqrt{s} \leq 1000 \text{ GeV}$. The parameters are chosen as $d_U = 1.1$, $\Lambda_U = 1000$ GeV. The figure shows that the total cross-section increases rapidly when the collision energy \sqrt{s} increases.

iii) In Fig.7, we evaluate the dependence of the total cross-section on the Λ_U at the fixed collision energy $\sqrt{s} = 500$ GeV. The cross-section decreases rapidly in the region of $1 \text{ TeV} \leq \Lambda_U \leq 3 \text{ TeV}$ and gradually in the region of $3 \text{ TeV} \leq \Lambda_U \leq 5 \text{ TeV}$.

Some numerical values for the cross sections are given detaily in Table 2. The results show that in the $\gamma\gamma \rightarrow W^- W^+$ subprocess, the cross-sections are about 10^3 times larger than that of the W - pair production without the scalar unparticle propagator, however the cross-sections are much smaller than that in the $e^+ e^-$ collision. With the integrated luminosity of the order of $L = 100 \text{ fb}^{-1}$ yearly [27], the number of events are given in detail in Table 3, which shows that with the contribution of the scalar unparticle, the W - pair production cross-sections may give the observable values at ILC with the low values of the scaling dimension (d_U is close to 1) and the bounds on scale Λ_U are around few TeV.

IV Conclusion

In this paper, we have evaluated the influence of the scalar unparticle on the W - pair production cross-sections at ILC in the RS model. Numerical evaluations show that the cross section of the W -

pair production depends strongly on the collision energy \sqrt{s} , the scaling dimension d_U of the unparticle operator \mathcal{O}_U and also the energy scale Λ_U . The results indicate that with the contribution of the scalar unparticle, the cross-sections are enhanced and much larger than the pair production of scalar particles [20] under the same conditions, which may give the observable values at ILC. It is worth noting that the W mode at e^+e^- colliders is possible to discover the existence of the unparticle with the low values of the scaling dimension and the bounds on scale Λ_U are around few TeV. Note that some phenomenology of the scalar unparticle was discussed in Ref. [28] which showed that the UnCasimir effect could provide the strongest bounds on some restricted region of the unparticle parameter space (d_U very close to 1).

Finally, we emphasize that the W mode is the simplest one to study the effect of the scalar unparticle at ILC, this is due to W - pair can only be produced through the s - channel in the unparticle case.

Acknowledgements: The work is supported in part by the National Foundation for Science and Technology Development (NAFOSTED) of Vietnam under Grant No. 103.01-2016.44.

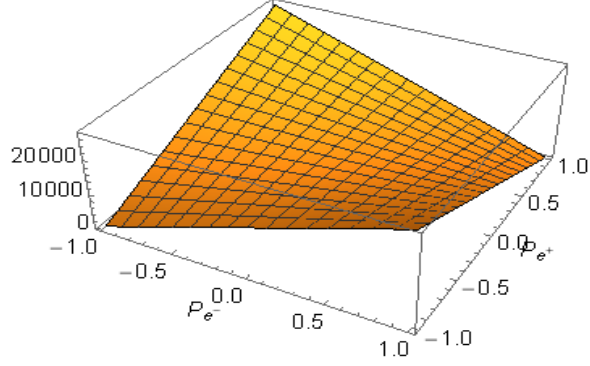


Figure 1: The cross-section as a function of the P_{e^-}, P_{e^+} polarization coefficients of the e^-, e^+ beams at ILC. The parameters are taken to be $\sqrt{s} = 500$ GeV, $d_U = 1.1$, $\Lambda_U = 1000$ GeV, respectively.

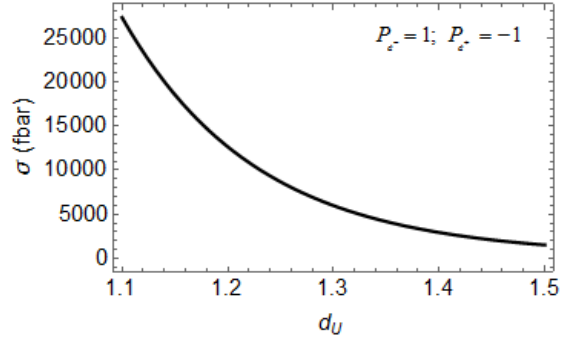


Figure 2: The cross-section as a function of the d_U in $e^+e^- \rightarrow W^-W^+$ collision in case of $P_{e^-} = 1$, $P_{e^+} = -1$. The parameters are chosen as $\sqrt{s} = 500$ GeV, $\Lambda_U = 1000$ GeV.

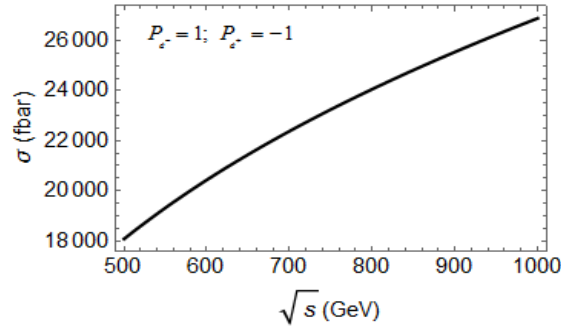


Figure 3: The cross-section as a function of the collision energy \sqrt{s} in $e^+e^- \rightarrow W^-W^+$ collision in case of $P_{e^-} = 1$, $P_{e^+} = -1$. The parameters are chosen as $d_U = 1.1$, $\Lambda_U = 1000$ GeV.

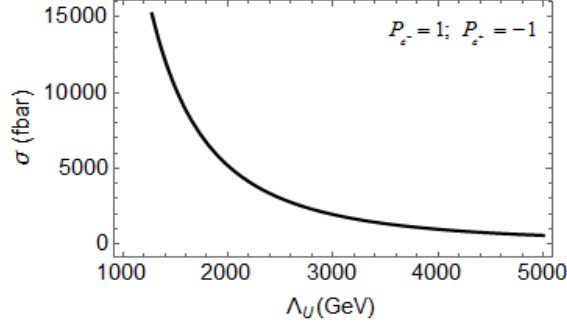


Figure 4: The total cross-section as a function of the energy scale Λ_U in $e^+e^- \rightarrow W^-W^+$ collision in case of $P_{e^-} = 1, P_{e^+} = -1$. The parameters are taken to be $\sqrt{s} = 500$ GeV, $d_U = 1.1$.

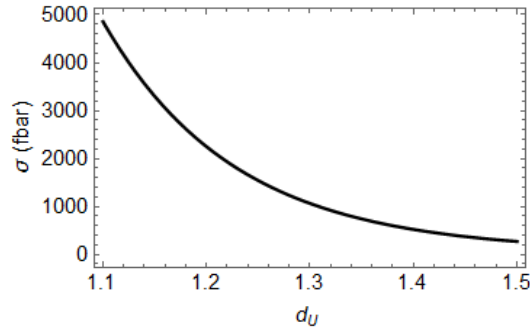


Figure 5: The cross-section as a function of the d_U in $\gamma\gamma \rightarrow W^-W^+$ subprocess. The parameters are chosen as $\sqrt{s} = 500$ GeV, $\Lambda_U = 1000$ GeV.

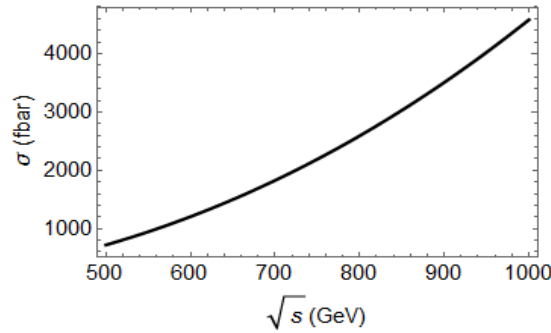


Figure 6: The cross-section as a function of the collision energy \sqrt{s} in $\gamma\gamma \rightarrow W^-W^+$ subprocess. The parameters are chosen as $d_U = 1.1, \Lambda_U = 1000$ GeV.

Table 1: Some typical values for the cross-section with the contribution of the scalar unparticle in the $e^+e^- \rightarrow W^-W^+$ collisions at the ILC in case of $P_{e^-} = 1, P_{e^+} = -1$. The parameters are chosen as $d_U = 1.1$ and the masses $m_h = 125$ GeV, $m_\phi = 10$ GeV.

\sqrt{s} (GeV)	500	600	700	800	900	1000
$\sigma(e^+e^- \xrightarrow{\phi, h} W^-W^+) (10^{-7} \text{ fbar})$	5.287	5.320	5.343	5.358	5.369	5.378
$\sigma(e^+e^- \xrightarrow{\phi, h, U} W^-W^+) (\text{fbar})$	18070.8	20431.3	22381.8	24061.5	25549.8	26895.4

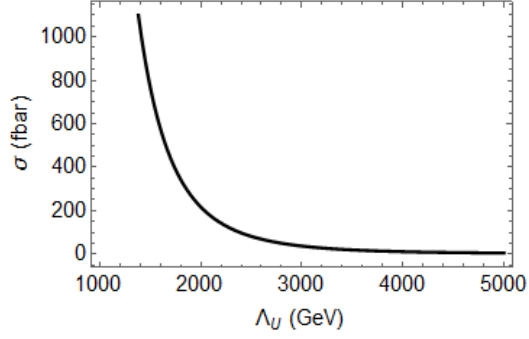


Figure 7: The total cross-section as a function of the energy scale Λ_U in $\gamma\gamma \rightarrow W^-W^+$ subprocess. The parameters are taken to be $\sqrt{s} = 500$ GeV, $d_U = 1.1$.

Table 2: Some typical values for the cross-section with the contribution of the scalar unparticle in the $\gamma\gamma \rightarrow W^-W^+$ subprocess at the ILC. The parameters are chosen as $d_U = 1.1$ and the masses $m_h = 125$ GeV, $m_\phi = 10$ GeV.

\sqrt{s} (GeV)	500	600	700	800	900	1000
$\sigma_{sub} (\gamma\gamma \xrightarrow{\phi,h} W^-W^+) \text{ (fbar)}$	0.299	0.442	0.612	0.809	1.032	1.287
$\sigma_{sub} (\gamma\gamma \xrightarrow{\phi,h,U} W^-W^+) \text{ (fbar)}$	720.54	1206.34	1828.06	2593.29	3509.31	4582.99

Table 3: The number of events in a year with some different values of the collision energy. The parameters are chosen as $d_U = 1.1$ and the masses $m_h = 125$ GeV, $m_\phi = 10$ GeV, the luminosity $L = 100 fb^{-1}$ yearly (ILC).

\sqrt{s} (GeV)	500	600	700	800	900	1000
N ($e^+e^- \xrightarrow{\phi,h,U} W^-W^+$) (10^6)	1.807	2.043	2.238	2.406	2.555	2.689
N ($\gamma\gamma \xrightarrow{\phi,h,U} W^-W^+$) (10^5)	0.721	1.206	1.828	2.593	3.509	4.583

References

- [1] H. Zhang, C. S. Li and Z. Li, *Phys. Rev.* **D76** (2007) 116003.
- [2] K. Cheung, W. Y. Keung and T. C. Yuan, *Phys. Rev. Lett.* **99** (2007) 051803.
- [3] H. Georgi, *Phys. Rev. Lett.* **98** (2007) 221601.
- [4] H. Georgi, *Phys. Lett.* **B650** (2007) 275.
- [5] T. Banks and A. Zaks, *Nucl. Phys.* **B196** (1982) 189.
- [6] S-L. Chen, X-G. He, *Phys. Rev.* **D76** (2007) 091702.
- [7] CMS Collaboration, *Eur. Phys. J.* **C75** (2015) 235.
- [8] CMS Collaboration, *Phys. Rev.* **D93** (2016) 052011.
- [9] P. Mathews and V. Ravindran, *Phys. Lett.* **B657** (2007) 198.
- [10] A.T. Alan and N.K. Pak, *EPL* **Vol.84**, No.1 (2008) 11001.
- [11] S. Majhi, *Phys. Lett.* **B665** (2008)44.
- [12] M.C. Kumar, P. Mathews, V.Ravindran and A.Tripathi, *Phys. Rev.* **D77** (2008) 055013.
- [13] I. Sahin and B. Sahin, *Eur. Phys. J.* **C55** (2008) 325.
- [14] T.Kikuchi and N.Okada, *Phys. Rev.* **D77** (2008) 094012.
- [15] A. Friedland, M. Giannotti, M. Graesser, *Phys. Lett.* **B678** (2009) 149.
- [16] E. O. Iltan, *Eur. Phys. J.* **C56** (2008) 105.
- [17] C. H. Chen, G. Cvetič, C. S. Kim, *Phys. Lett.* **B694** (2011)393.
- [18] S. Khatibi, M. M. Najafabadi, *Phys. Rev.* **D87** (2013) No.3, 037701.
- [19] T.M. Aliev, S. Bilmis, M. Solmaz and I. Turan, *Phys. Rev.* **D95** (2017) No.9, 095005.
- [20] D. V. Soa and B. T. H. Giang, *Nucl. Phys.* **B 936** (2018) 1.
- [21] L. Randall and R. Sundrum, *Phys. Rev. Lett.* **83** (1999) 3370.
- [22] D. Dominici, B. Grzadkowski, J. F. Gunion and M. Toharia, *Nucl.Phys.* **B671** (2003) 243.
- [23] A. Ahmed, B. M. Dillon, B. Grzadkowski, J. F. Gunion and Y. Jiang, *Phys. Rev.* **D95** (2017) 095019.
- [24] M. E. Peskin and D. V. Schroeder, *An Introduction to Quantum Field Theory*, Addison-Wesley Publishing (1995).
- [25] D. V. Soa *et al.*, *Mod. Phys. Lett.* **A27** (2012)1250126.
- [26] I. F. Ginzburg, G. L. Kotkin, V. G. Serbo and V. I. Telnov, *Nucl. Instr. and Meth.* **205** (1983) 47; I. F. Ginzburg, G. L. Kotkin, S. L. Panfil, V. G. Serbo and V. I. Telnov, *Nucl. Instr. and Meth.* **219** (1984) 5; V. I. Telnov, *Nucl. Phys. Proc. Suppl* **82** (2000) 359.

- [27] N. Sonmez, *Phys. Rev. D.* **91** (2014) 085021.
- [28] Antonia M. Frassino, Piero Nicolini and Orlando Panella, *Phys. Lett.* **B772** (2017)675.
- [29] C. Csaki, M. L. Graesser and G. D. Kribs, *Phys. Rev.* **D63** (2001) 065002.
- [30] W. D. Goldberger and M. B. Wise, *Phys. Rev. Lett.* **83** (1999) 4922.